Journal of Advanced Research 32 (2021) 1–14

Contents lists available at ScienceDirect

Journal of Advanced Research

journal homepage: www.elsevier.com/locate/jare

Original Article

Finite-time stabilization of a perturbed chaotic finance model

Israr Ahmad [a], Adel Ouannas [b], Muhammad Shafiq [c], Viet-Thanh Pham [d,*], Dumitru Baleanu [e,f,g]

[a] Department of General Requirements, University of Technology and Applied Sciences, College of Applied Sciences, Nizwa, Oman
[b] Department of Mathematics and Computer Science, University of Larbi Ben M'hidi, Oum El Bouaghi
[c] Department of Electrical and Computer Engineering, Sultan Qaboos University, Oman
[d] Nonlinear Systems and Applications, Faculty of Electrical and Electronics Engineering, Ton Duc Thang University, Ho Chi Minh City, Viet Nam
[e] Department of Mathematics, Cankaya University, Ankara, Turkey
[f] Department of Medical Research, China Medical University Hospital, & China Medical University Taichung, Taiwan
[g] Institute of Space Sciences, Magurele-Bucharest, Romania

HIGHLIGHTS

- This article proposes a new robust nonlinear controller that stabilizes a chaotic finance system in a finite-time without cancellation of the spacecraft's nonlinear terms, it improves the efficiency of the closed-loop.
- It accomplishes an oscillation-free faster convergence of the perturbed state variables to the desired steady-state.
- The proposed controller is insensitive to the parameter uncertainties of the nonlinear terms and exogenous disturbances.
- The paper performs a comparative study to verify the performance and efficiency of the proposed controller.

GRAPHICAL ABSTRACT

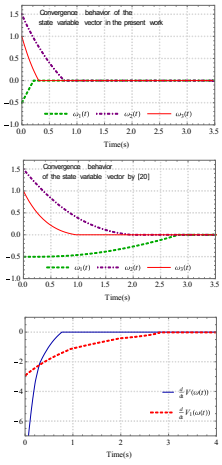

ARTICLE INFO

Article history:
Received 27 June 2020
Revised 27 May 2021
Accepted 12 June 2021
Available online 16 June 2021

Keywords:
Chaotic finance system
Nonlinear control
Chaos suppression
Lyapunov function
Finite-time stability

ABSTRACT

Introduction: Robust, stable financial systems significantly improve the growth of an economic system. The stabilization of financial systems poses the following challenges. The state variables' trajectories (i) lie outside the basin of attraction, (ii) have high oscillations, and (iii) converge to the equilibrium state slowly.

Objectives: This paper aims to design a controller that develops a robust, stable financial closed-loop system to address the challenges above by (i) attracting all state variables to the origin, (ii) reducing the oscillations, and (iii) increasing the gradient of the convergence.

Methods: This paper proposes a detailed mathematical analysis of the steady-state stability, dissipative characteristics, the Lyapunov exponents, bifurcation phenomena, and Poincare maps of chaotic financial dynamic systems. The proposed controller does not cancel the nonlinear terms appearing in the closed-loop. This structure is robust to the smoothly varying system parameters and improves closed-loop efficiency. Further, the controller eradicates the effects of inevitable exogenous disturbances and accomplishes a faster, oscillation-free convergence of the perturbed state variables to the desired steady-state within a finite time. The Lyapunov stability analysis proves the closed-loop global stability.

Peer review under responsibility of Cairo University.

* Corresponding author.
E-mail addresses: ouannas.adel@univ-oeb.dz (A. Ouannas), phamvietthanh@tdtu.edu.vn (V.-T. Pham), dumitru@cankaya.edu.tr (D. Baleanu).

https://doi.org/10.1016/j.jare.2021.06.013

The paper also discusses finite-time stability analysis and describes the controller parameters' effects on the convergence rates. Computer-based simulations endorse the theoretical findings, and the comparative study highlights the benefits.

Results: Theoretical analysis proofs and computer simulation results verify that the proposed controller compels the state trajectories, including trajectories outside the basin of attraction, to the origin within finite time without oscillations while being faster than the other controllers discussed in the comparative study section.

Conclusions: This article proposes a novel robust, nonlinear finite-time controller for the robust stabilization of the chaotic finance model. It provides an in-depth analysis based on the Lyapunov stability theory and computer simulation results to verify the robust convergence of the state variables to the origin.

Introduction

Many systems in nature and social sciences exhibit chaotic behavior. Generally, chaotic systems are highly sensitive to the initial conditions and parameter variations [1]. Chaotic systems display predictable random-like behavior, which may produce undesired system performance [2]. These inadmissible characteristics motivate research communities to either reduce or eliminate the effects of chaos and employ these systems for industrial and technological advancement [3]. For example, the dynamics of many systems appearing in science, engineering, economics, politics, and the environment owe chaotic behavior [4–6]. The coronary artery system exhibits both regular and chaotic dynamics. Chaotic behavior in the coronary artery system occurs due to myocardial infraction that gives birth to cardiopathy and other arrhythmia diseases [7]. The investigation of chaos stabilization in the coronary artery system is to diagnose and propose a treatment that reduces cardiopathy risk and diminishes other arrhythmia problems [4]. Mobile robots encounter several complex challenges, including vibrations, noise-sensing generation, and irregular robot-environmental interfaces during the execution of a particular task. These nonlinearities generate chaos in mobile robots that cause failure to complete the mission [8]. The main objective of chaos suppression in mobile robots is to eliminate the chaotic behavior to complete the task [8]. Chaos occurs in artificial satellites due to the perturbation torque acting on them; it moves the spacecraft away from the desired stable orbit [9]. The main objective for controlling chaos in an artificial satellite system is to stabilize the satellite's attitude motion in the desired orbit [9]. The DC-DC converter is a type of power electronic circuit used in everyday electronic equipment. The fluctuations in the voltage, external disturbances, and uncertainties in the components' values produce chaos in the DC-DC converter [10]. The existence of chaos affects the performance of the DC-DC converter in practice, including faults in actuation. Chaos suppression in the DC-DC converter aims to run the system at a desirable low frequency and rejecting fault tolerance [10]. Similarly, [11] describes the chaotic behavior of the single-machine-infinite bus power system, and [12] proposes four feedback controllers for the chaotic permanent magnet synchronous motor that make the closed-loop characteristics independent of the initial operational conditions. [13] designs a controller to address issues related to the non-fragile memory filtering in Takagi–Sugeno (T-S) fuzzy delayed neural networks with randomly occurring time-varying parameters uncertainties and variable sampling rates. A reliable asynchronous sampled-data T-S fuzzy controller is proposed in [14] that assures the asymptotic stability of the uncertain delayed neural networks with stochastically switched topologies. Though [13] and [14] consider the stochastic environment but adopt a chaotic system control strategy in designing the controller.

Researchers in different fields developed various feedback control strategies for controlling the chaos appearing in the above applications, such as backstepping control design [15], switched fuzzy sampled-data control [16], sliding mode control method [17], H_∞ control strategy [18], adaptive control technique [19], and nonlinear controller [20], (among others). These control techniques are applied to achieve either asymptotic stability [19] or finite-time stability [20] of the closed-loops. In the asymptotic stability, the state trajectories of a chaotic system converge to the origin as $t \to \infty$, while the finite-time stability accomplishes the control of chaos in finite-time. The finite-time control methodologies demonstrate faster convergence of the state variables to zero than the asymptotic stabilization control strategies; they show better disturbance rejection characteristics and higher precision performance [21]. These attributes of the finite-time controllers have many benefits in practical applications [22–24].

Chaos occurs in nonlinear finance models that exhibit complex behavior due to inherent randomness in economic factors [25]. Change of interest rates due to external forces, environmental interferences, fluctuations in the exchange rates, sudden changes in the stock market prices, and other economic factors, including political policies and news, alter the saving amount in a financial model that transforms the financial system's periodic dynamics into chaotics [26–28]. The presence of chaos in real economic and financial systems reveals that the macroeconomic operations have inherent uncertainties that produce economic growth disturbances, leading to financial system crises [27]. Chaos in the financial system poses difficulties in short-medium-long term predictions and financial systems planning [28]. The primary purpose of chaos stabilization in a financial system is to maintain the saving amount to a certain level that restores the economic cycle's normalization; it helps in management and decision-making strategies [29]. Therefore, it is desirable to design control strategies to reduce or eliminate the chaotic phenomenon in the financial systems to improve the economic system's predictability [29]. Chaos in the dynamics of the financial and economic models motivates researchers that develop efficient control algorithms to suppress hyper(chaos) in various financial models. [30] investigates the control of chaos in the chaotic finance model (CFM) [25] using the Pyragas feedback control scheme [31]. A nonlinear state-feedback controller is designed in [32] to study the finite-time control of a CFM. By adding a fourth state variable (marginal profit) to the CFM proposed in [25], the chaotic phenomena of a new hyperchaotic system are discussed in [33]. The article [33] designs linear feedback and speed feedback controllers that achieve hyperchaos suppression of the CFM. [34] use the linear matrix inequality technique based on the Lyapunov functional method and Jensen inequality approach to discussing the control of a CFM in the presence of input time-delay and exogenous disturbances. Based on Pontryagin's maximum principle [35] and using the optimal

control theory, [36] stabilizes the hyperchaotic finance model proposed in [33] to the equilibrium point at the origin. In the paper [36], an adaptive control algorithm has also been extended to control the uncertain hyperchaotic finance model. [37] investigates a new hyperchaotic finance system and discusses its chaotics based on its parameter variations. In [37], a modified adaptive control algorithm is proposed that realizes the stabilization and synchronization of the proposed hyperchaotic finance model with uncertain parameters. [38] designs a nonlinear finite-time adaptive controller and discusses the finite-time stabilization of third-order and fourth-order chaotic finance systems with and without market confidence. A linear matrix inequality technique based on the Lyapunov second theorem of stability, finite-time stability theory, and the Wirtinger inequality technique is proposed in [39] to investigate the finite-time H_∞ control of a CFM. The energy-bounded exogenous disturbances and time-delay perturb the CFM in [39]. Most recently, [40] proposes a robust resilient fault-tolerant guaranteed cost controller with delay to tackle the fluctuations in investment policy scheme with minimum guaranteed cost bound. The article [40] also discusses the finite-time control of hyperchaos in a CFM.

Challenges and motivations

The following items delineate a summary of the challenges.

(i) The control algorithms in [29,30,33,34,37] achieve the asymptotic stabilization of the hyper(chaotic) finance model at the origin. It creates two challenges; (a) if the initial state variables of the controlled system lie outside the basin of attraction, the state trajectories may not converge to the targeted equilibrium point, and (b) it generates rapid and uneven fluctuations in the financial market that affect economic growth and activities [40].
(ii) The paper [32] discusses the finite-time control of CFM using the feedback linearization concept. The feedback linearization methods employ the nonlinear terms cancelation technique. Generally, the closed-loop structures formed by the feedback linearization methods generate high oscillations in the transient phase. The oscillations in state variables trajectories are the sources of several undesirable attitudes in the CFM [40], such as the fast fluctuations in the cash flow and labor force. Further, the control input signal in the finite-time controller (FTC) function [32,38] comprises a feedback component $\omega^p(t)$ $(0 < p < 1)$, where $\omega(t)$ represents the state variables vector. However, $\omega^p(t) \in C$ when $\omega(t) < 0$. This attribute of the FTC scheme makes it an infeasible solution.
(iii) The controllers proposed in [29,30,32–34,36–40] show slower convergence rates of the state variables vector to the origin.

Table 1 summarizes the contributions of the recent research in CFM control [30,32–34,36–40] and describes future research directions that emerge from these state-of-the-art developments.

The above challenges motivate the design of feedback controllers to stabilize a financial system that develops a closed-loop structure with the following properties to prevent socio-economic crises and unrest.

(i) The state variables converge to the desired steady-state in a finite time.
(ii) The fast convergence rates of the state variables to the steady-state.
(iii) Better disturbance rejection.
(iv) Higher precision.

This paper proposes a control strategy and develops a methodology that establishes finite-time convergence of the state variable trajectories to the origin smoothly. The closed-loop response is faster and oscillation-free. Subsection 'Contributions' describes the contributions of the proposed controller.

Contributions

This article proposes and analyzes a novel FTC design to address the above challenges having the properties given in motivation items (i) to (iii). This novel FTC consists of four nonlinear feedback components that make the closed-loop stable, converge the state variables to the desired steady-state in a finite time, and eradicate the effect of time-varying exogenous disturbances and parameter variations. The upper bound of the finite-time convergence is robust. It is the main contribution of the paper, as discussed in Section 'Proposed Finite-Time Controller'. Analysis based on the Lyapunov direct theorem [41] and finite-time stability theory [42] assures the global stabilization of the CFM at the origin in finite time. Computer-based simulation results validate the theoretical analysis.

Further, the closed-loop system analysis and the simulation results show the robust performance of the CFM for the smooth variations in the plant parameters. The proposed controller does not cancel the plant's nonlinear terms, and the synthesis of the control effort is independent of the nonlinear terms of the CFM. Therefore, the exogenous disturbances and smooth slow parameter variations do not affect the closed-loop stability performance. The paper provides an in-depth analysis, which shows that the closed-loop is finite-time stable. The stability analysis is based on the Lyapunov stability theory. It also assures that the stability of the closed-loop is robust to the disturbances and parameter uncertainties. The article discusses computer simulation results for the verification of the theoretical findings. Also, it compares the performance of the closed-loop with other state-of-the-art FTC methodology proposed in [20].

Preliminaries of chaotic finance model

This section illustrates the preliminaries of CFM.

Subsection 'Notations and symbols' provides notations and symbols used in this paper. Subsection 'Chaotic dynamics of the finance model' gives the dynamics of the CFM. In subsections 'Stability analysis of the balancing points', the article discusses chaos in the financial system and stability analysis at the balancing points. The dissipative characteristics and Lyapunov exponents of the CFM are discussed in subsections 'Dissipative characteristic' and 'Lyapunov exponents and Kaplan-Yorke dimension', respectively. The bifurcation phenomena and Poincare analysis of the CFM are illustrated in subsections 'Chaotic analysis based on bifurcation theory' and 'Poincare analysis', respectively. Subsection 'Methodology for the finite-time analysis' describes the methodology for the finite-time analysis.

Notations and symbols

Table 2 describes the notation and symbols used in this paper.

Chaotic dynamics of the finance model

This paper considers the CFM proposed in [25]. The CFM is composed of four sub-components that include production, stock, money, and labor force. Equation (1) presents the mathematical model describing the chaotic dynamics of the finance model. The structure of the CFM (1) comprises three basic state variables;

Table1
Review of the state-of-the-art controllers.

References	Contributions and methodology	Controller	Proof of stability	Possible research direction(s)
Chen et.al [30]	Time-delay feedback controller, and uses computer simulations based verification of the closed-loop system	Appendix A	The paper does not describe the stability proof	i. Theoretical stability and performance analysis of the closed-loop ii. Study the effects of the disturbances and parameter variations iii. Robust analysis iv. Analysis of the rate of convergence
Wang et.al [32]	Finite-time controller, theoretical and simulations based verification, and evaluation of the closed-loop system	Appendix B	Finite-time stability using control Lyapunov function	i. Avoiding the cancellation of nonlinear terms in the closed-loop ii. Singularities issues in the neighborhood of zero iii. Study the effects of the disturbances and parameter variations iv. $\boldsymbol{\omega}^p(t) \in C$ when $\boldsymbol{\omega}(t) < 0$, and$0 < p < 1$
Yu et.al [33]	Construction of a new hyperchaotic finance system, state-feedback controller, asymptotic stabilization of the closed-loop, theoretical and simulations based verification and evaluation of the closed-loop system	Appendix C	Asymptotic stabilization of the closed-loop based on the Lyapunov stability theory	i. Avoiding the cancellation of nonlinear terms in the closed-loop ii. Study the effects of the disturbances and parameter variations iii. Robust analysis iv. Analysis of the rate of convergence
Zhao et.al [34]	Time-delay feedback controller, linear matrix inequality technique, asymptotic stabilization of the closed-loop	Appendix D	Robust stability of the closed-loop using the linear matrix inequality technique based on the Lyapunov functional method and Jensen inequality	i. Study the effects of the parameter variations ii. Analysis of the rate of convergence iii. Reducing the state variable trajectories oscillations
Cao [36]	Adaptive controller, asymptotic stabilization of the closed-loop, theoretical and simulations based verification, and evaluation of the closed-loop system	Appendix E	Asymptotic stabilization of the closed-loop based on the Lyapunov stability theory	i. Study the effects of the disturbances and parameter variations ii. Robust analysis iii. Avoiding the cancellation of nonlinear terms in the closed-loop iv. Analysis of the rate of convergence
Jajarmi et.al [37]	Construction of a new hyperchaotic finance system, Adaptive control, theoretical and simulations based verification, and evaluation of the closed-loop system	Appendix F	Asymptotic stabilization of the closed-loop based on the Lyapunov stability theory	i. Avoiding the cancellation of nonlinear terms in the closed-loop ii. Study the effects of the disturbances and parameter variations iii. Robustness iv. Analysis of the rate of convergence
Ma et al. [38]	Direct adaptive finite-time controller, theoretical and simulations based verification, and evaluation of the closed-loop system	Appendix G	Finite-time stabilization of the closed-loop based on the Lyapunov stability theory and finite-time stability technique	i. Singularities issues in the neighborhood of zero ii. Study the effects of the disturbances and parameter variations iii. $\boldsymbol{\omega}^p(t) \in C$ when $\boldsymbol{\omega}(t) < 0$, and$0 < p < 1$
Xu et al. [39]	Time-delay finite-time feedback controller, theoretical and simulations based verification, and evaluation of the closed-loop system	Appendix H	Stability of the closed-loop in finite-time using the linear matrix inequality technique based on the Lyapunov functional theory, Wirtinger-based inequality	i. Study the effects of the disturbances and parameter variations ii. Robustness iii. Reducing the state variable trajectories oscillations iv. Analysis of the rate of convergence
Harshavarthini et.al [40]	Design of a resilient fault-tolerant guaranteed cost controller with delay, finite-time stabilization of the closed-loop, and simulations based verification, and evaluation of the closed-loop system	Appendix I	Stability of the closed-loop in finite-time using the linear matrix inequality technique based on the Lyapunov functional theory	i. Study the effects of the disturbances and parameter variations ii. Robustness iii. Analysis of the rate of convergence

the interest rate $\omega_1(t)$, demand for investment $\omega_2(t)$, and the price index $\omega_3(t)$.

$$\omega(t) = \begin{cases} \dot{\omega}_1(t) = [\omega_2(t) - \eta_1]\omega_1(t) + \omega_3(t) \\ \dot{\omega}_2(t) = 1 - \eta_2\omega_2(t) - \omega_1^2(t) \\ \dot{\omega}_3(t) = -\eta_3\omega_3(t) - \omega_1(t) \end{cases} \tag{1}$$

The parameters $\eta_1 > 0$, $\eta_2 > 0$, and $\eta_3 > 0$ represent the saving amount, cost per investment, and elasticity of demand of commercial markets, alternatively. Contradiction in the investment market and structural adjustment in the price of goods influence the state variable $\omega_1(t)$. The rate of change of $\omega_2(t)$ is proportional to the inversion of the cost of investment, interest rate and rate of investment. The contradiction between supply and demand of the commercial market controls the variable $\omega_3(t)$; it also depends on inflation rates [25].

Stability analysis of the balancing points

Considering $\dot{\omega}_1(t) = \dot{\omega}_2(t) = \dot{\omega}_3(t) = 0$ gives the steady-state of (1).

$$\begin{cases} [\omega_2(t) - \eta_1]\omega_1(t) + \omega_3(t) = 0 \\ 1 - \eta_2\omega_2(t) - \omega_1^2(t) = 0 \\ -\eta_3\omega_3(t) - \omega_1(t) = 0 \end{cases} \tag{2}$$

The solution of (2) gives the balancing points of the CFM (1).

$$\omega_{e1} = \left[0, \frac{1}{\eta_2}, 0\right], \omega_{e2,3} = \left[\pm\sqrt{1 - \eta_1\eta_2 - \frac{\eta_2}{\eta_3}}, \left(\eta_1 + \frac{1}{\eta_3}\right), \mp\frac{1}{\eta_3}\sqrt{1 - \eta_1\eta_2 - \frac{\eta_2}{\eta_3}}\right]$$

Table 2
Notation and symbols.

Symbols	Description
R	Real numbers
T	Transpose of a matrix/vector
$\omega(t) = [\omega_1(t), \omega_2(t), \omega_3(t)]^T \in R^{3\times1}$	State variables vector of the CFM (1)
η_1, η_2, andη_3	The constant parameters of the CFM (1)
$\Lambda(t) = [\Lambda_1(t), \Lambda_2(t), \Lambda_3(t)]^T \in R^{3\times1}$	Time-varying exogenous disturbances acting on the CFM (12)
$\mathbf{u}(t) = [u_1(t), u_2(t), u_3(t)]^T \in R^{3\times1}$	Control input vector
$\boldsymbol{\alpha} = [\alpha_{ij}, i,j = 1,2,3, i\neq j \Rightarrow \alpha_{ij} = 0] \in R^{3\times3}$,	Feedback controller gains
$\boldsymbol{\beta} = [\beta_{ij}, i,j = 1,2,3, i\neq j \Rightarrow \beta_{ij} = 0] \in R^{3\times3} \boldsymbol{\gamma} = [\gamma_{ij}, i,j = 1,2,3, i\neq j \Rightarrow \gamma_{ij} = 0] \in R^{3\times3}$	
$\sigma \in R$, $0 < \sigma < 1$	Controller parameter
e	The base of the natural Logarithm
$\text{sign}(\omega(t)) = \begin{cases} 1 & \omega(t) \in R^+ \\ -1 & \omega(t) \in R^- \end{cases}$	Signum function
$\lvert a\rvert$	The absolute value of a scalar$a \in R$
$\lvert\mathbf{b}\rvert = [\lvert b_1\rvert, \lvert b_2\rvert, \cdots, \lvert b_n\rvert]^T$	The absolute of a vector $\mathbf{b} \in R^{n\times1}$, where $b_i \in \mathbf{b}$ for $i \in (1,2,\cdots,n)$
$\lVert\mathbf{b}\rVert = \sum_1^n \lvert b_i\rvert$	Norm-1 of$\mathbf{b}$
$\lVert\mathbf{b}\rVert_2 = \left(\sum_1^n b_i^2\right)^{\frac{1}{2}}$	Norm-2 of$\mathbf{b}$

The authors in [25] give a detailed discussion about the stability and bifurcation of these balancing points.

This paper considers $\eta_1 = 0.9, \eta_2 = 0.2$, and $\eta_3 = 1.2$ in the simulation examples by following [26,33]. Stability and bifurcation of these balancing points as follows.

The Jacobian matrix of the CFM (1) is given below.

$$\boldsymbol{J}_{\omega(t)} = \begin{bmatrix} -0.9 + \omega_2(t) & \omega_1(t) & 1 \\ -2\omega_1(t) & -0.2 & 0 \\ -1 & 0 & -1.2 \end{bmatrix} \tag{3}$$

Table 3 summarizes the stability analysis of the CFM (1) balancing points.

Dissipative characteristic

The existence of a strange attractor in a nonlinear or infinite-dimensional dynamical system assures chaos in the system [43]. A dynamic system is dissipative if the vector field's divergence is negative.

Following (1), let us consider the vector field $\mathbf{v}$ as:

$$\mathbf{v} = \begin{bmatrix} \dot{\omega}_1(t) \\ \dot{\omega}_2(t) \\ \dot{\omega}_3(t) \end{bmatrix} = \begin{bmatrix} \omega_1(t)\omega_2(t) - 0.9\omega_1(t) + \omega_3(t) \\ 1 - 0.2\omega_2(t) - \omega_1^2(t) \\ -1.2\omega_3(t) - \omega_1(t) \end{bmatrix} \tag{4}$$

The divergence of (4) is given by:

$$\nabla.\mathbf{v} = \frac{\partial(\omega_1(t)\omega_2(t) - \eta_1\omega_1(t) + \omega_3(t))}{\partial\omega_1(t)} + \frac{\partial\left(1 - 0.2\omega_2(t) - \omega_1^2(t)\right)}{\partial\omega_2(t)} + \frac{\partial(-1.2\omega_3(t) - \omega_1(t))}{\partial\omega_3(t)}$$

$$= \omega_2(t) - 0.9 - 0.2 - 1.2 = -(\omega_2(t) + 2.3) \tag{5}$$

Table 3
Stability analysis of CFM (1).

i	ω_{ei}	$\lambda_{ij}, i,j = 1,2,3$	Analysis
1	$[0,5,0]$	$\lambda_{11} = 3.894$, $\lambda_{12} = -1.0037$, $\lambda_{13} = -0.2$	The system is unstable at ω_{e1} (saddle-focus)
2	$[0.83, 1.57, -0.55]$	$\lambda_{21,22} = 0.093 \pm 1.36i$, $\lambda_{23} = -0.916$	The system is unstable at ω_{e2} (saddle-focus)
3	$[-0.83, 1.57, 0.55]$	$\lambda_{31,32} = 0.093 \pm 1.36i$, $\lambda_{33} = -0.916$	The system is unstable at ω_{e3} (saddle-focus)

The system (1) is dissipative for $\omega_2(t) > -2.3$; it means that each volume element $V_0 e^{-(\omega_2(t)+2.3)t}$ containing the trajectories of the system (1) shrinks to zero at an exponential rate $(\omega_2(t) + 2.3)$ as $t \to \infty$. Therefore, trajectories of the CFM (1) are attracted by a strange attractor. Hence, system (1) is chaotic.

Lyapunov exponents and Kaplan-Yorke dimension

The Lyapunov exponents [44] provide a quantitative measure of the divergence or convergence of the nearby trajectories for a dynamical system. The Lyapunov exponent measures sensitive dependence on initial conditions at $t = 0$ and is calculated based on how rapidly two nearby states diverge from each other. The Lyapunov exponents of (1) are $LE_1 = 0.000$, $LE_2 = 0.0180$, and $LE_3 = -0.2127$.

Now

$$0.000 + 0.0180 - 0.2127 = -0.1947 < 0 \tag{6}$$

Therefore, system (1) is chaotic [44].

The Lyapunov dimension of CFM (1) is computed by the Kaplan-Yorke conjecture,

$$D_{KY} = j + \frac{\sum_{i=1}^{j} LE_j}{\lvert LE_{j+1}\rvert} = 2 + \frac{LE_1 + LE_2}{\lvert LE_3\rvert} = 2.0846 \tag{7}$$

which is fractional. Consequently, system (1) is chaotic [45].

Fig. 1 illustrates the 3D chaotic attractor, Fig. 2 demonstrates the state variables' behavior, and Fig. 3. depicts the 2D phase portraits of the system (1), when $\eta_1 = 0.9, \eta_2 = 0.2$, and $\eta_3 = 1.2$.

Chaotic analysis based on bifurcation theory

Variations in the parameter values cause qualitative changes in the system dynamics, referred to as bifurcation; the points at which these qualitative changes occur are known as bifurcation points [46]. Fig. 4 shows that all the equilibrium points follow higher order bifurcation periods due to the variations in the system parameter η_3. This behavior of the bifurcation plots confirms that system (1) exhibits chaotic dynamics.

Poincare analysis

The Poincare section technique [46] investigates the behavior of a continuous dynamical system for projecting higher dimensions trajectories into two dimensions; the system exhibits a chaotic phenomenon when a dense limit cycle of the state space trajecto-

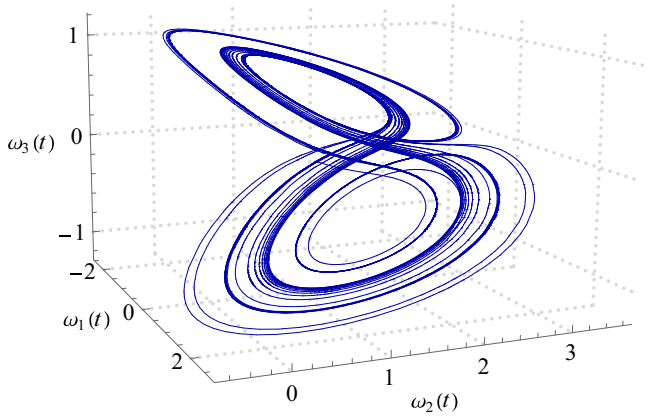

Fig. 1. (a) 3-D phase portrait.

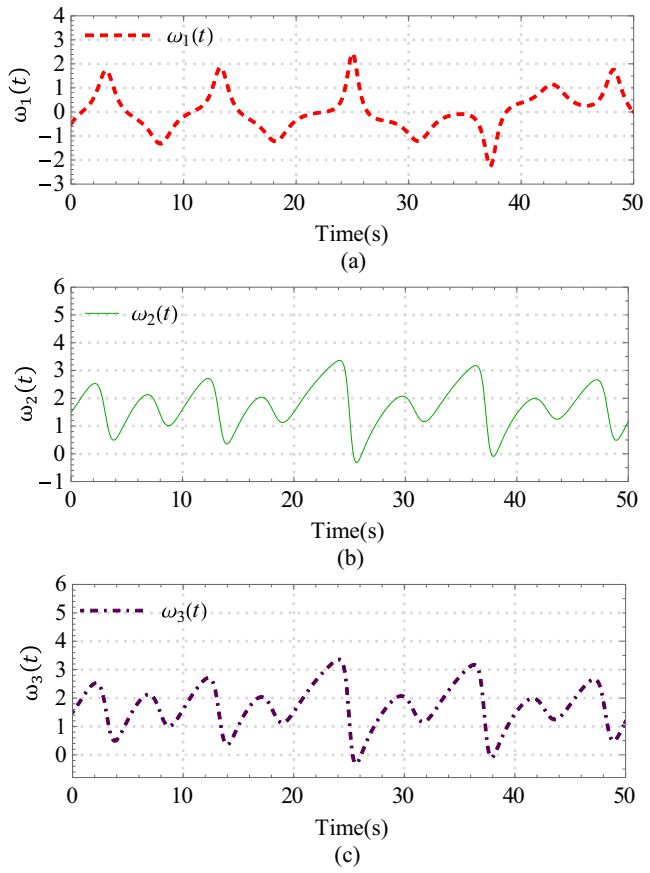

Fig. 2. Chaotic behavior of the states.

ries on a 2-D section has a limit cycle; otherwise, it shows a periodic orbit. Fig. 5 illustrates the Poincare sections of the system (1), (a) $\omega_1(t)vs\ \omega_2(t)$, (b) $\omega_1(t)vs\ \omega_3(t)$, and (c) $\omega_2(t)vs\ \omega_3(t)$, alternatively.

Methodology for the finite-time analysis

This subsection describes the finite-time convergence analysis framework for a nonlinear dynamic system based on the Lyapunov function.

Lemma 1 [47]. *Consider* $V(t):[0,\infty)\to[0,\infty)$ *be a Lyapunov function described in* (8).

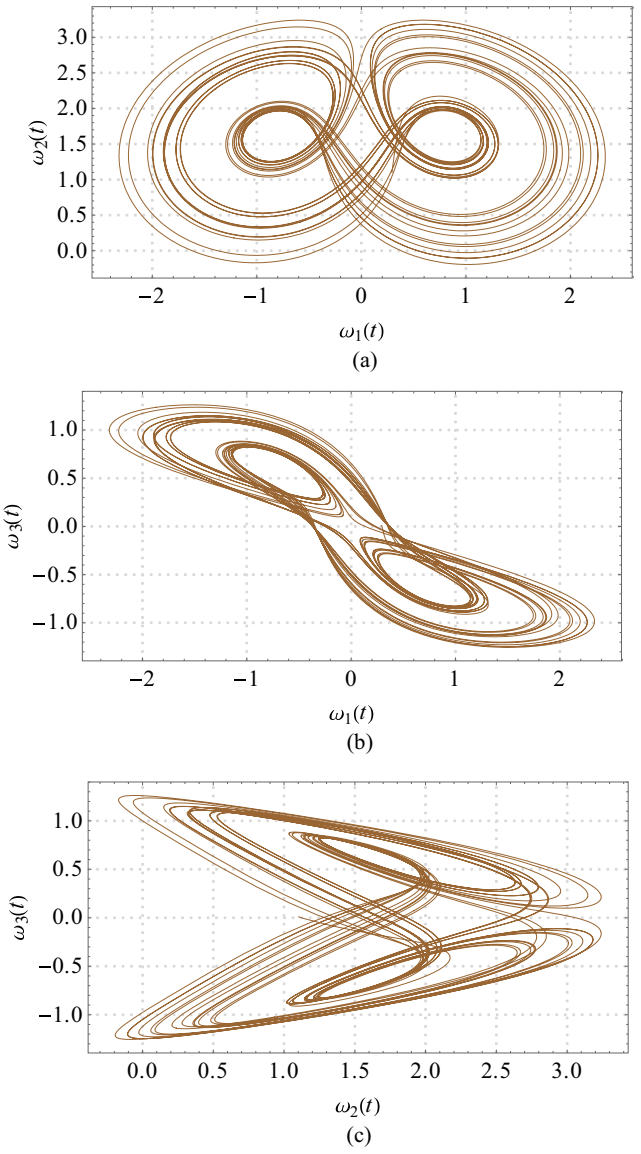

Fig. 3. 2-D phase portraits (a) $\omega_1(t)vs\ \omega_2(t)$, (b) $\omega_1(t)vs\ \omega_3(t)$, and (c).$\omega_2(t)vs\omega_3(t)$.

$$\begin{cases} \dot{V}(t) \le -\kappa V^p(t), \text{and} \\ 0 \le V(t_0), t_0 \le t, \end{cases} \tag{8}$$

where t_0 *is the initial time, and* $\kappa, p \in R$ *such that* $\kappa > 0$, *and* $0 < p < 1$.
Equation (9) *gives the solution of* (8).

$$\begin{cases} V^{1-p}(t) \le V^{1-p}(t_0) - (t-t_0)(1-p)\kappa, \text{for } t_0 \le t \le \tau, \text{ and} \\ V(t) = 0, \forall t_0 \le t. \end{cases} \tag{9}$$

In (10), τ *is the time such that if* $V(t_0) > 0$, *then* $\lim_{t\to\tau} V(t) = 0$, *and*

$$\tau \le \tau_1 = t_0 + \frac{V^{1-p}(t_0)}{(1-p)\kappa} \tag{10}$$

where κ *regulates the finite-time convergence rates and* $\tau_1 \in R^+$.
The following remark drives the relationship in (10).

Remark 1 [48]. For $\lim_{t\to\tau} V(t) = 0$, Eq. (9) gives:

$$\tau(1-p)\kappa \le V^{1-p}(t_0) + \kappa(1-p)t_0$$

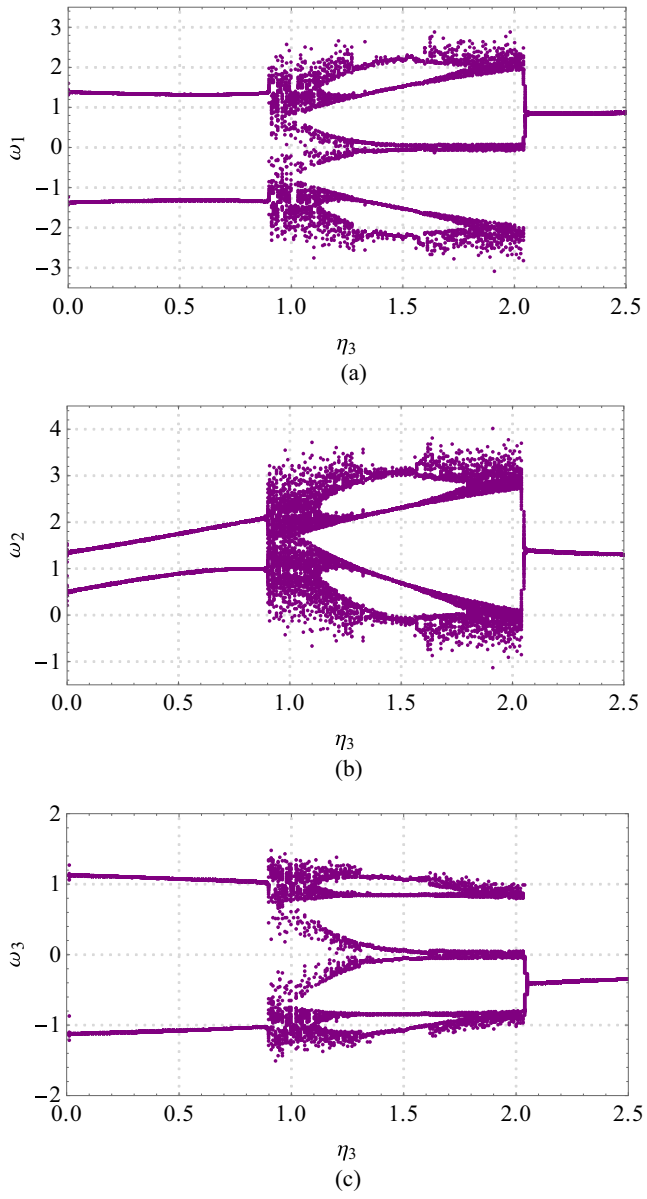

Fig. 4. Bifurcation of states with parameter η_3 (a) $\eta_3 vs\ \omega_1$, (b) $\eta_3 vs\ \omega_2$, and (c)$\eta_3 vs \omega_3$.

$$\Rightarrow \tau \le \tau_1 = t_0 + \frac{V^{1-p}(t_0)}{(1-p)\kappa} \tag{11}$$

If $V(t_0)$, t_0, τ_1, and p are known, then it is easy to compute $\kappa \le \frac{V^{1-p}(t_0)}{(\tau - t_0)(1-p)}$

Problem description

When exogenous disturbances $\Lambda_i(t)$ and control efforts $u_i(t)$ act on the CFM (1), then (12) represents the closed-loop dynamics.

$$\begin{cases} \dot{\omega}_1(t) = [\omega_2(t) - \eta_1]\omega_1(t) + \omega_3(t) + \Lambda_1(t) + u_1(t) \\ \dot{\omega}_2(t) = 1 - \eta_2\omega_2(t) - \omega_1^2(t) + \Lambda_2(t) + u_2(t) \\ \dot{\omega}_3(t) = -\eta_3\omega_3(t) - \omega_1(t) + \Lambda_3(t) + u_3(t) \end{cases} \tag{12}$$

In this scenario, it is desired to design a feedback controller for synthesizing control effort $\mathbf{u}(t) \in R^{3\times 1}$ that forces the state of the closed-loop system (12) to the origin in finite time.

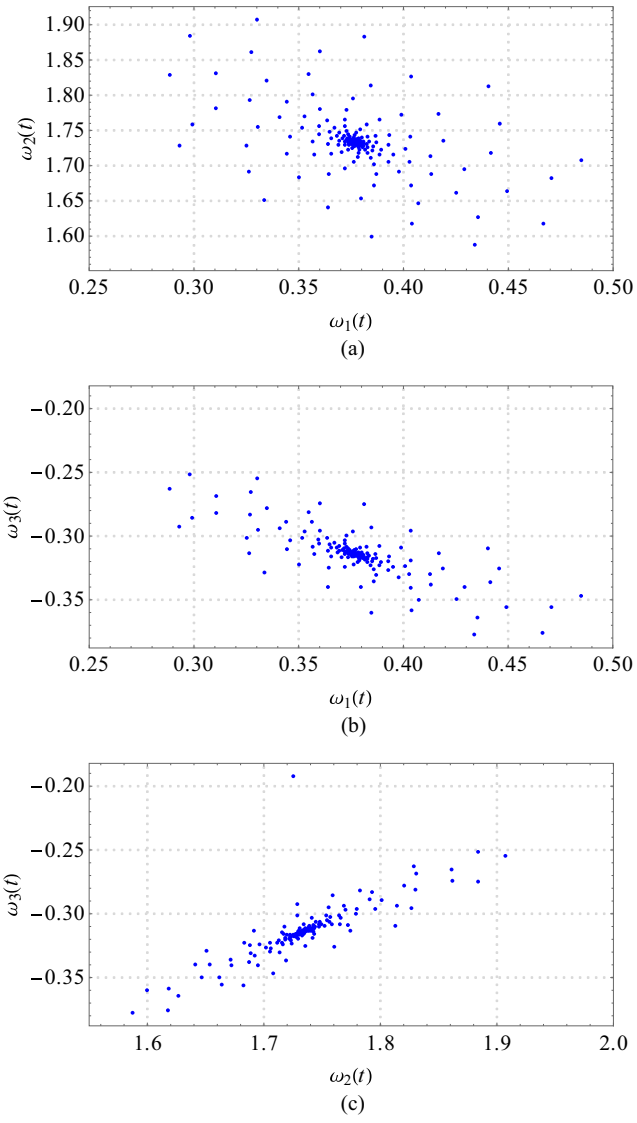

Fig. 5. Poincare maps (a) $\omega_1(t) vs\ \omega_2(t)$, (b) $\omega_1(t) vs\ \omega_3(t)$, and (b).$\omega_2(t) vs \omega_3(t)$.

Assumption 1. The exogenous disturbances caused by environmental interference influence the financial and economic chaotic models [34]; it may destabilize systems, resulting in undesirable behavior. This paper assumes that the bounded exogenous disturbances $\Lambda_i(t)$ act upon CFM (12). Therefore, there exists an upper bound $\varphi_i \in R^+$ of the disturbances such that:

$$|\Lambda_i(t)| \le \varphi_i, \quad i \in (1,2,3) \tag{13}$$

Assumption 2. The influence of the economic factors such as supply-demand, fluctuations in the prices and cost of demand; the parameters $\eta_1 \in R^+$, $\eta_2 \in R^+$, and $\eta_3 \in R^+$ of the CFM (1) vary during the financial activities in the market [37].

Proposed finite-time controller

The presence of chaos in a financial system prevents policymakers from predicting and analyzing future economic trends. This feature of a financial system brings an economic crunch in the financial cycle [33]. Therefore, it is necessary to eliminate the chao-

tic financial system phenomena in a finite time to make long-term future predictions that establish healthy economic activities and growth [28]. Most of the literature discusses the asymptotic stability of the CFM. Timely prediction of the financial system behavior is a requirement for planning and management; the asymptotic stability of a CFM does not develop a good base for predicting the rapid fluctuations in the financial system that affects economic growth. These issues urge to design of a controller that suppresses the chaos in the CFM in a finite time.

Eq. (14) introduces a new FTC design that stabilizes the closed-loop (12) at the origin in finite time.

$$\mathbf{u}(t) = \begin{cases} u_i(t) = -\alpha_i\psi_i(t)\omega_i(t) - (\Omega_i(t) + \varphi_i)\text{sgn}(\omega_i(t)), i = 1,3 \\ u_2(t) = -\alpha_2\psi_2(t)\omega_2(t) - (\Omega_2(t) + \varphi_2)\text{sgn}(\omega_2(t)) - 1, \end{cases} \tag{14}$$

where $\Omega(t) = diag[\gamma_i\psi_i(t) + \beta_i]$, where $\psi_i(t) = e^{-\sigma|\omega_i(t)|}$.

If $\omega_i(t) > 0$, then $\text{sgn}(\omega_i(t)) = 1$, if $\omega_i(t) < 0$, then $\text{sgn}(\omega_i(t)) = -1$, and if $\omega_i(t) \neq 0$, then $\text{sgn}(\omega_i(t)) = \frac{\omega_i(t)}{|\omega_i(t)|}$ for $i = 1,2,3$.

Items (i)-(iii) summarize the role of distinct components of the control input (14).

(i) $\alpha_i\psi_i(t)\omega_i(t)$ makes the closed-loop globally stable; it assures the converges of the state variables to the origin.

(ii) $(\gamma_i\psi_i(t) + \beta_i)\text{sgn}(\omega_i(t))$ realizes oscillation free, smooth, and rapid convergence of the state variables to zero and establishes finite-time stabilization. The parameter σ regulates the decay rate. The simulation results depicted in Fig. 6 validates it.

(iii) $\varphi_i\text{sgn}(\omega_i(t))$ eradicates the effects of time-varying exogenous disturbances.

Analysis of the closed-loop

This section analyzes two claims; (a) the perturbed state variables converge to the equilibrium point of the closed-loop, and (b) converges of the state variables completes in finite time. Theorem 1 limns it.

Theorem 1. *FTC (14) computes control effort* $\mathbf{u}(t)$. *It is an input signal to the CFM (12). Application of* $\mathbf{u}(t)$ *to the CFM (12) establishes convergence of the state variables vector* $\omega(t)$ *to the origin in finite-time* τ *as given in (15).*

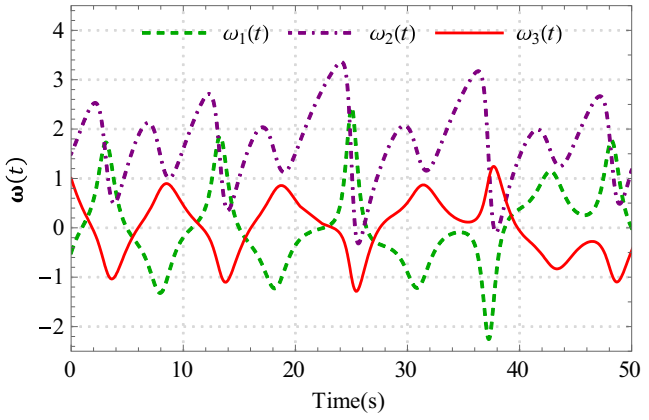

Fig. 6. (a). The behavior of the state variables $\omega_i(t)$, $i = 1,2,3$ without control input Fig. 6. (b). The convergence of the state variables $\omega_i(t)$, $i = 1,2,3$ to zero when $\sigma = 0.01$, $\alpha_i = \beta_i = \gamma_i = 1$ Fig. 6 (c). The convergence of the state variables $\omega_i(t)$, $i = 1,2,3$ to zero when $\sigma = 5$,$\alpha_i = \beta_i = \gamma_i = 1$.

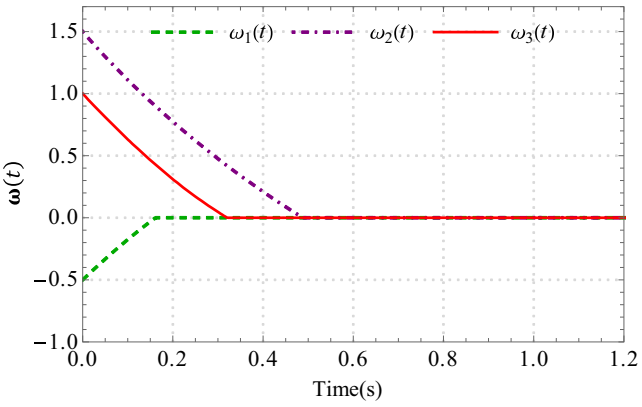

Fig. 6 (*continued*)

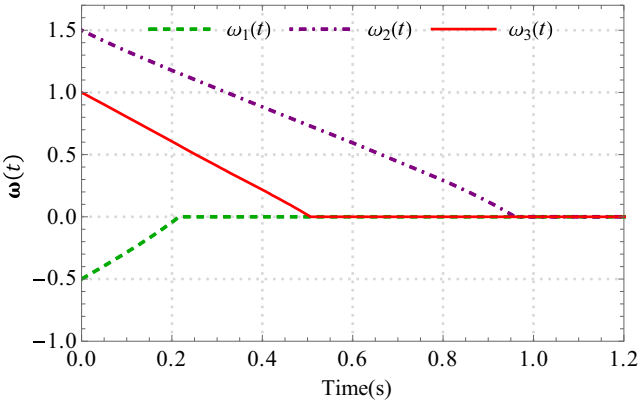

Fig. 6 (*continued*)

$$\tau \leq \tau_1 = \frac{\|\omega(0)\|_2}{\beta_m} \tag{15}$$

where $\beta_m = Minimum(\beta_i)$, and $0 < \tau \leq \tau_1 \in R^+$ represents the finite time. τ depends on the initial conditions $\omega(0) = [\omega_1(0), \omega_2(0), \omega_3(0)]^T$ and the controller parameter β_m.

Subsection 'Analysis of the state trajectories convergence' proves the convergence of the closed-loop state variables based on the Lyapunov direct analysis theorem for global asymptotic stability [49]. Theorem 1 assures the finite-time convergence, and subsection 'Proof of Theorem 1' describes its proof.

Analysis of the state trajectories convergence

Consider the following quadratic and positive definite function:

$$V(\omega(t)) = \frac{1}{2}\omega^T(t)\omega(t) \geq 0 \tag{16}$$

The derivative of (16) along (12) implies:

$$\begin{aligned} \tfrac{dV(\omega(t))}{dt} &= \omega_1(t)([\omega_2(t) - \eta_1]\omega_1(t) + \omega_3(t) + \Lambda_1(t) + u_1(t)) \\ &+\omega_2(t)\big(1 - \eta_2\omega_2(t) - \omega_1^2(t) + \Lambda_2(t) + u_2(t)\big) \\ &+\omega_3(t)(-\eta_3\omega_3(t) - \omega_1(t) + \Lambda_3(t) + u_3(t)) \\ &= \omega_1^2(t)\omega_2(t) - \eta_1\omega_1^2(t) + \omega_1(t)\omega_3(t) + \Lambda_1(t)\omega_1(t) + \omega_1(t)u_1(t) \\ &+\omega_2(t) - \eta_2\omega_2^2(t) - \omega_1^2(t)\omega_2(t) + \Lambda_2(t)\omega_2(t) + \omega_2(t)u_2(t) \\ &-\eta_3\omega_3^2(t) - \omega_1(t)\omega_3(t) + \Lambda_3(t)\omega_3(t) + \omega_3(t)u_3(t). \end{aligned} \tag{17}$$

Apply the controller (14) to (17) yields:

$$\frac{dV(\omega(t))}{dt} = -\sum_{1}^{3}\eta_i\omega_i^2(t) + \sum_{1}^{3}\Lambda_i(t)\omega_i(t) - \sum_{1}^{3}\alpha_i\psi_i(t)\omega_i^2(t) - \sum_{1}^{3}(\Omega_i(t)+\varphi_i)\mathrm{sgn}(\omega_i(t))\omega_i(t)$$

$$\leq -\sum_{1}^{3}(\alpha_i\psi_i(t)+\eta_i)\omega_i^2(t) + \sum_{1}^{3}\Lambda_i(t)|\omega_i(t)| - \sum_{1}^{3}\Omega_i(t)\mathrm{sgn}(\omega_i(t))\omega_i(t) - \varphi_i\mathrm{sgn}(\omega_i(t))\omega_i(t). \quad (18)$$

Using Assumption 1 and the fact $\mathrm{sgn}(\omega_i(t))\omega_i(t) = |\omega_i(t)|$ to (18) implies:

$$\frac{dV(\omega(t))}{dt} \leq -\sum_{1}^{3}(\alpha_i\psi_i(t)+\eta_i)\omega_i^2(t) - \sum_{1}^{3}\Omega_i(t)|\omega_i(t)| \quad (19)$$

Remark 2. According to the Lyapunov theory, Eqs. (16) and (19) guarantee that the closed-loop is globally asymptotically stable provided $(\alpha_i\psi_i(t)+\eta_i) > 0$, $\gamma_i\psi_i(t) > 0$ and $\beta_i > 0$. It assures the convergence of the state variables to the equilibrium point.

Remark 3. Assume that $L_{1i}(t) = \alpha_i\psi_i(t) + \eta_i$, and $L_{2i}(t) = \gamma_i\psi_i(t)$. Choosing $L_{1i}(t) > 0$, $L_{2i}(t) > 0$, and $\beta_i > 0$ is sufficient to satisfy inequality (19). The speed of convergence increases for larger values of $L_{1i}(t) > 0$, $L_{2i}(t) > 0$, and $\beta_i > 0$; it is evident from Fig. 7.

Remark 4. As the plant parameters $\eta_i \in R^+$; therefore, the closed-loop stability is insensitive to the variation of these parameters. Thus, the closed-loop performance is robust to the smooth variations of the CFM (1) parameters. Fig. 8 illustrates this finding.

Proof of Theorem 1

Let us proceed by using (19)

$$\frac{dV(\omega(t))}{dt} \leq -\sum_{1}^{3}(\alpha_i\psi_i(t)+\eta_i)\omega_i^2(t) - \sum_{1}^{3}\gamma_i\psi_i(t)|\omega_i(t)| - \sum_{1}^{3}\beta_i|\omega_i(t)|$$

$$\leq -\sum_{1}^{3}\beta_i|\omega_i(t)| \leq 0$$

Further,

$$\frac{dV(\omega(t))}{dt} \leq -Minimum(\beta_i)\|\omega(t)\|_1 = -\beta_m\|\omega(t)\|_2 = -\beta_m\sqrt{\frac{2\omega^T(t)\omega(t)}{2}} = -\sqrt{2}\beta_m(V(\omega(t)))^{\frac{1}{2}} \leq 0$$

Hence

$$\frac{dV(\omega(t))}{dt} \leq -\sqrt{2}\beta_m(V(\omega(t)))^{\frac{1}{2}} \quad (20)$$

Using the finite-time convergence analysis framework in subsection 'Methodology for the finite-time analysis', Eq. (20) gives:

$$\tau \leq \tau_1 = \frac{\|\omega(0)\|_2}{\beta_m} \quad (21)$$

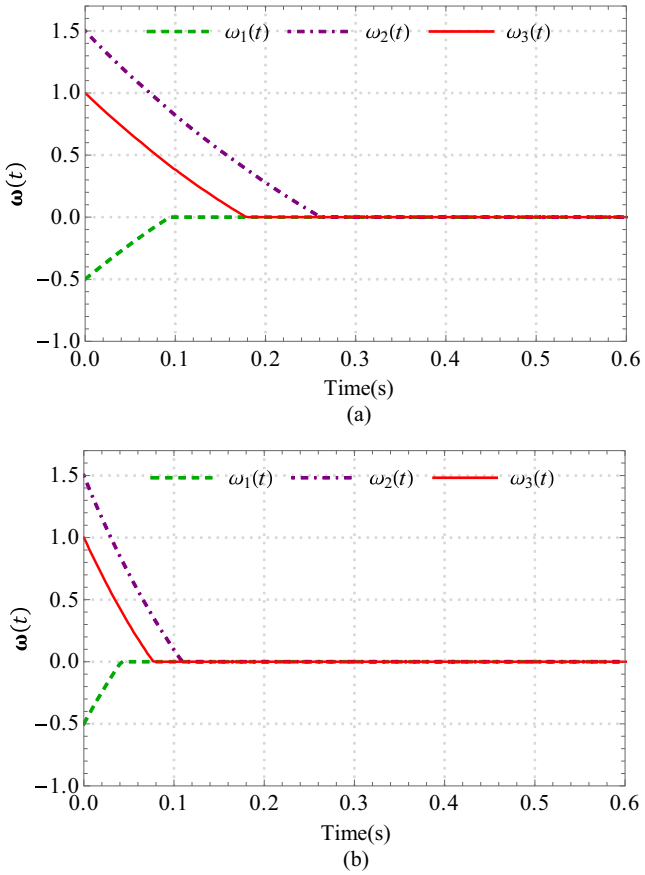

Fig. 7. The convergence behavior of the state variables when (a) $\alpha_i = \beta_i = \gamma_i = 2, \sigma = 0.01$, and (b)$\alpha_i = \beta_i = \gamma_i = 5, \sigma = 0.01$.

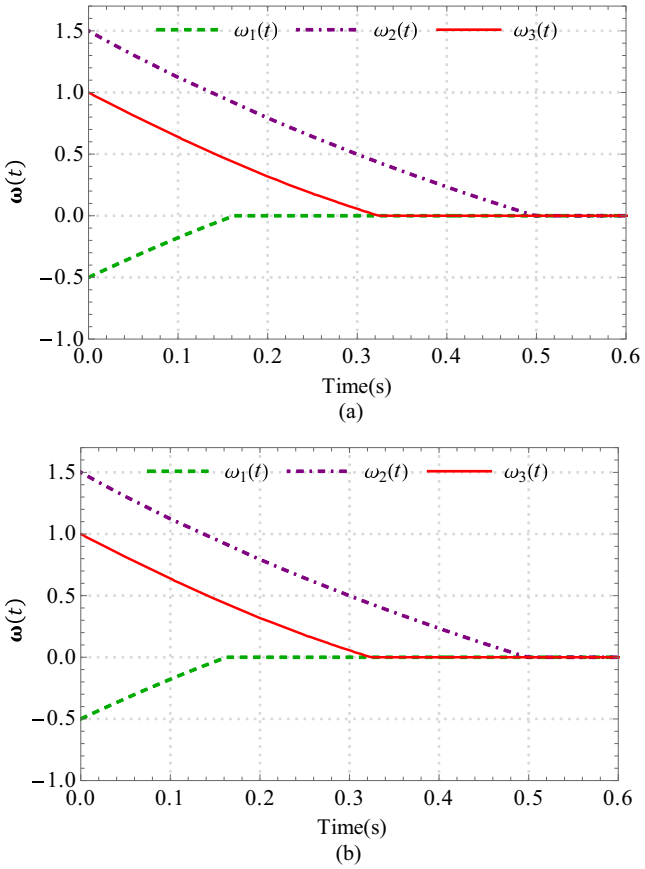

Fig. 8. The convergence behavior of the state variables for (a) Example 2, (b) Example 3.

Remark 5. The upper bound of the time of convergence is a function of initial conditions $[\omega_1(0), \omega_2(0), \omega_3(0)]^T$ and the controller parameter β_m.

This completes the proof of Theorem 1.

Numerical simulations and comparative study

All the simulations are performed by considering the parameters and initial conditions given in Table 4. This paper uses Mathematica 12.0 version in the Microsoft 10 environment for all the simulations. The numerical solution of the dynamic systems is performed using the fourth-order Runge-Kutta method with step size 0.001. The truncation error in the fourth-order Runge-Kutta method is of order-four $O\left(h^4\right)$, where h represents the step size and O is the order. It is a widely used method for the numerical solution of differential equations [50,51].

Fig. 6(a) demonstrates the behavior of the state variables $\omega_i(t)$, $i \in (1,2,3)$ without any control effort. It shows that the state variable trajectories keep oscillating in a bounded region. This behavior is a consequence of the chaotics, as discussed in Section 'Preliminaries of Chaotic Finance Model'.

Example 1. In this example, parameters of the financial system are fixed, and no exogenous disturbance exists.

The convergence behavior of the state variables depicted in Fig. 6(b) is achieved using the proposed FTC (14) by selecting $\sigma = 0.01$. It illustrates that all converge to zero in less than 0.48 s smoothly. Fig. 6(c) demonstrates the convergence behavior for $\sigma = 4$. Results in Fig. 6(b) and (c) conclude that for larger values of controller parameter σ, the convergence behavior becomes slow, while in both cases, trajectories remain smooth.

Fig. 7 illustrates that the convergence of the state variable trajectories become faster when the values of gains α_i, β_i, and γ_i are large. This observation is shown in Fig. 7. In Fig. 7(a), $\alpha_i = \beta_i = \gamma_i = 2$ and Fig. 7(b), $\alpha_i = \beta_i = \gamma_i = 5$. In Fig. 7(a) and (b), all the trajectories converge to zero in less than 0.26 and 0.14 s, respectively.

Robustness analysis of the closed-loop

The influence of the economic factors such as supply-demand, fluctuations in the prices, and cost of demand; the positive parameters η_1, η_2, and η_3 of the CFM (1) vary due to the variations in the financial market activities. Similarly, the exogenous disturbances caused by environmental interference influence the financial and economic chaotic models [34]; it may destabilize systems, resulting in undesirable behavior. Therefore, to analyze the robustness of the proposed FTC (14), this subsection discusses the convergence behavior of the state variable trajectories to the origin when the CFM (1) parameters change smoothly and expose to the various exogenous disturbances acting on the system.

Table 4
Initial conditions and parameters for simulations.

Initial conditions	CFM parameters	Controller parameters
$\omega_1(0) = -0.5$	$\eta_1 = 0.9$	$\alpha_1 = \beta_1 = \gamma_1 = 1, \sigma = 0.01$
$\omega_2(0) = 1.5$	$\eta_2 = 0.2$	$\alpha_2 = \beta_2 = \gamma_2 = 1, \sigma = 0.01$
$\omega_3(0) = 1$	$\eta_3 = 1.5$	$\alpha_3 = \beta_3 = \gamma_3 = 1, \sigma = 0.01$

Effects on the performance of the closed-loop due to the smooth system parameter variations

This subsection discusses effects on the convergence time due to smooth variations in the system parameters between 0.1 and 1.

Example 2. Parameter variations in this example are:

$$\eta_1 = 0.9 - 0.2\cos 5t, \eta_2 = 0.2 - 0.2\cos 5t, \text{and } \eta_3 = 1.2 - 0.2\cos 5t \quad (23a)$$

Example 3. Parameter variations in this example are:

$$\eta_1 = 0.9 - 0.1e^{\sigma t}, \eta_2 = 0.2 - 0.1e^{\sigma t}, \text{and } \eta_3 = 1.2 - 0.1e^{\sigma t} \quad (23b)$$

Fig. 8 (a) and (b) demonstrate the convergence of state variables to the equilibrium point for Examples 2 and 3, respectively. Table 5 summarizes the convergence time behavior.

Impact of the exogenous disturbances on the closed-loop performance

The following two examples describe the effects of the exogenous disturbances [52–54] on the convergence time on the state variable trajectories.

Example 4. Exogenous disturbances are selected as:

$$\Lambda_i(t) = 0.3\sin 0.5\frac{\pi}{6}t, i = 1,2,3 \quad (24a)$$

Example 5. Exogenous disturbances are selected as:

$$\Lambda_i(t) = 0.1\cos\left(0.5\pi t + \frac{\pi}{6}\right), i = 1,2,3 \quad (24b)$$

Fig. 9 (a) and (b) depict that the convergence time remains less than the upper bound of the finite time computed as a function of initial conditions in the presence of the exogenous disturbances. The summary of the convergence time is given in Table 5.

Effects of both parameter variations and exogenous disturbances

Examples in this subsection discuss the combined effect of the parameter variations and exogenous disturbances on the convergence time of the state variable trajectories.

Example 6. This example considers parameters variations $\eta_i(t)$ and exogenous disturbances $\Lambda_i(t)$, which are given in (25a) and (25b), respectively.

$$(i) \quad \eta_1 = 0.9 - 0.2\cos 5t, \eta_2 = 0.2 - 0.2\cos 5t, \text{ and } \eta_3 = 1.2 - 0.2\cos 5t \quad (25a)$$

Table 5
Comparative results for the convergence time to zero.

Example No.	Figure No.	Parameter variations	Convergence time	Example No.	Figure No.	Exogenous disturbances	Convergence time
2	8(a)	Eq. (23a)	$t = 0.5s$	4	9(a)	Eq. (24a)	$t = 0.54s$
3	8(b)	Eq. (23b)	$t = 0.48s$	5	9(b)	Eq. (24b)	$t = 0.54s$
Example No.		Figure No.		Parameter variations and exogenous disturbances		Convergence time	
6		10(a)		Eqs. (23a) and (24a)		$t = 0.78s$	
7		10(b)		Eqs. (23b) and (24b)		$t = 0.68s$	

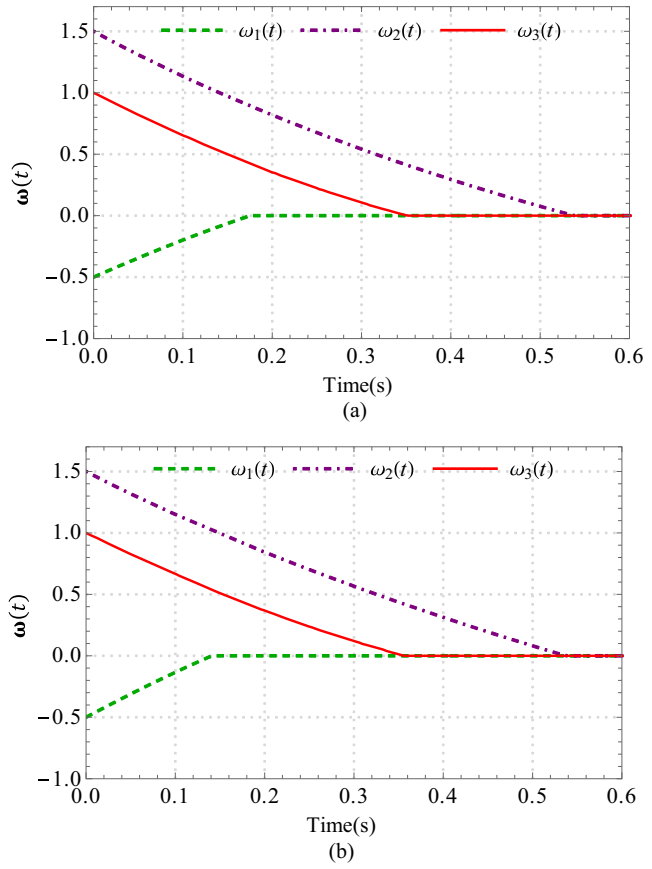

Fig. 9. The convergence behavior of the state variables in the presence of exogenous disturbances (a) Example 4, and (b) Example 5.

$$(ii) \quad \Lambda_i(t) = 0.3\sin 0.5\frac{\pi}{6}t, i = 1,2,3 \tag{25b}$$

Example 7. Parameter variations and exogenous disturbances in this example are:

$$(i) \quad \eta_1 = 0.9 - 0.1e^{\sigma t}, \eta_2 = 0.2 - 0.1e^{\sigma t}, \text{ and } \eta_3 = 1.2 - 0.1e^{\sigma t} \tag{26a}$$

$$(ii) \quad \Lambda_i(t) = 0.5\cos\left(0.5\pi t + \frac{\pi}{6}\right), i = 1,2,3 \tag{26b}$$

Fig. 10 (a) and (b) show that the convergence time is 0.78 seconds and 0.68 seconds, respectively. The summary of all simulation results is given in Table 5.

Data in Table 5 verifies that state variable trajectories in all examples converge to the equilibrium point in less than the upper bound of the finite-time convergence. These examples describe that smooth parameter variation and bounded exogenous disturbances do not destabilize the closed-loop and the convergence time follows the design finite-time bound.

Comparative study

The following examples are chosen from the paper [20] to analyze the comparative performance and efficiency of the proposed FTC (14). Assume that initial conditions and controller design parameters are the same for both systems for benchmarking.

Example 8:. This example re-simulates Example 1 using the controller proposed in [20] and described by (27).

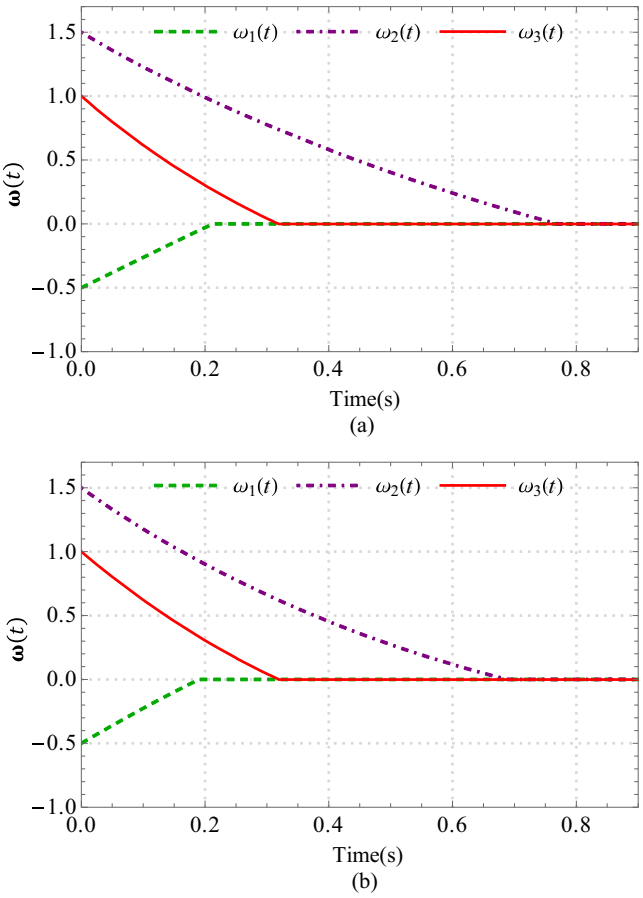

Fig. 10. The convergence behavior of the state variables in the presence of parameters variations and exogenous disturbances, (a) Example 6, and (b) Example 7.

$$\begin{cases} u_1(t) = -\omega_1(t)\omega_2(t) - \omega_3(t) - \alpha_1\omega_1^p(t) \\ u_2(t) = -1 + \omega_1^2(t) - \alpha_2\omega_2^p(t) \\ u_3(t) = \omega_1(t) - \alpha_3\omega_3^p(t) \end{cases} \tag{27}$$

where $0 < p < 1$ is any positive real constant.

Fig. 11 depicts the transient behavior of the state variable vector trajectories by FTC (27). Fig. 11 demonstrates that the state variables $\omega_i(t), i = 1,2,3$ do not show convergence behavior.

This paper modifies FTC (27) by introducing $\varphi_i \text{sgn}(\omega_i(t))$ as described in (28), this modification makes the closed-loop stable

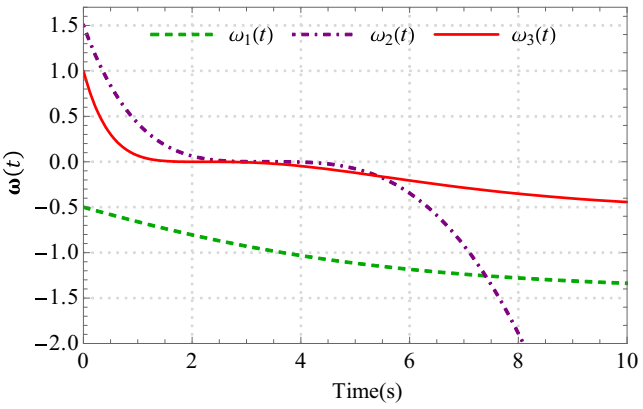

Fig. 11. The convergence behavior of the state variables using the control effort (27).

hence eliminates the diverging behavior. Now, the closed-loop is suitable for the comparative study.

$$\begin{cases} u_1(t) = -\omega_1(t)\omega_2(t) - \omega_3(t) - \alpha_1\omega_1^p(t) - \varphi_1 \mathrm{sgn}(\omega_1(t)) \\ u_2(t) = -1 + \omega_1^2(t) - \alpha_2\omega_2^p(t) - \varphi_2 \mathrm{sgn}(\omega_2(t)) \\ u_3(t) = \omega_1(t) - \alpha_3\omega_3^p(t) - \varphi_3 \mathrm{sgn}(\omega_3(t)) \end{cases} \quad (28)$$

Example 9. This example considers the same parameter variations and exogenous disturbances as given in (23a) and (24a), respectively.

Fig. 12(a) shows that the time of convergence of state variable trajectories to the equilibrium point is longer than the proposed FTC (14), and it is greater than the upper bound of the finite-time defined in (15).

Example 10. When parameters variations $\eta_i(t)$ and exogenous disturbances $\Lambda_i(t)$ are used as given in (23b) and (24b), respectively.

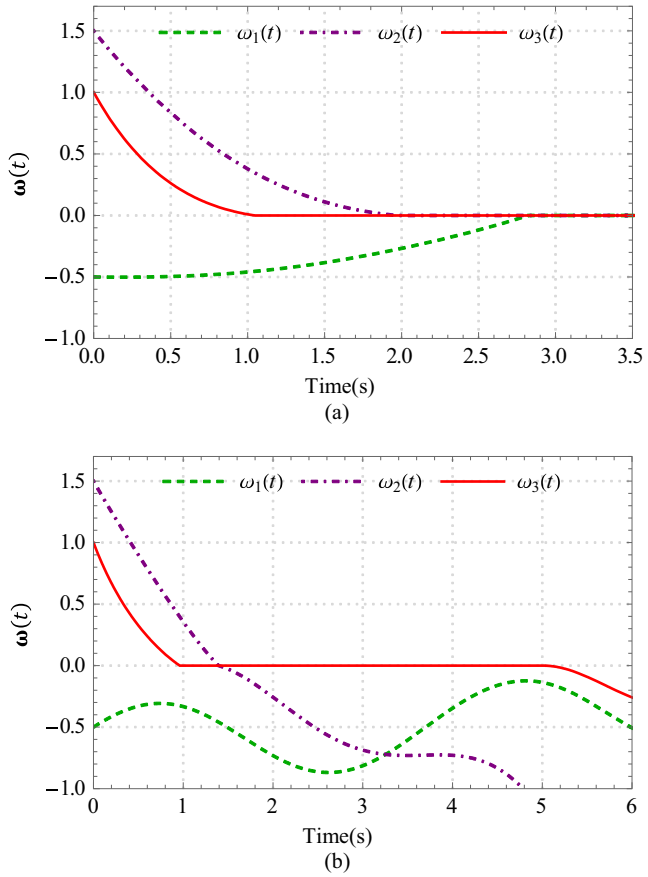

Fig. 12. The convergence behavior of the state variables using the control effort (28), (a) Example 9, and (b) Example 10.

The state variable trajectories in Fig. 12(b) do not converge.

The analysis of these simulation results concludes that the proposed algorithm is more robust to the smooth parameter variations and exogenous disturbances than [20].

Subsection 'Analysis and conclusion of the computer simulations' briefly describes the analysis of the simulation results and conclusions with some remarks.

Analysis and conclusion of the computer simulations

The gradient of the energy function associated with the state variable trajectories of the closed-loops developed by the proposed FTC (14) and FTC in [20] are given in Table 7. Here energy function terminology is used for the Lyapunov function in subsection 'Analysis of the state trajectories convergence'.

In Table 7, $V(\omega(t)) = V_1(\omega(t))$, and the gradients are given in (29).

$$\frac{d}{dt}V(\omega(t)) \le \frac{d}{dt}V_1(\omega(t)). \quad (29)$$

The simulation results depicted in Fig. 13 verify the inequality (29). Fig. 13 and inequality (29) affirm that the proposed controller (14) accomplishes faster convergence of energy function $V(\omega(t))$ to zero than the other controller (28). It confirms that the proposed controller (14) uses lesser energy than the controller (28). Further, in the vicinity of zero, $\frac{d}{dt}V(\omega(t))$ approaches zero that assures the smoothness and oscillation-free behavior of the steady-state.

Table 8 reports and compares convergence time between Examples 1 and 8, Examples 6 and 9, and Examples 7 and 10. This table shows that the proposed controller (14) establishes convergence of the state variable vector in all cases faster than the controller in [20]. Further, the closed-loop formed by the controller in [20] diverges for some initial conditions, parameter variations, and exogenous disturbances. It concludes that the proposed controller (14) develops a closed-loop, which is energy-efficient, and convergence of the state variables is fast, oscillation-free, and robust to the parameter variations and exogenous disturbances.

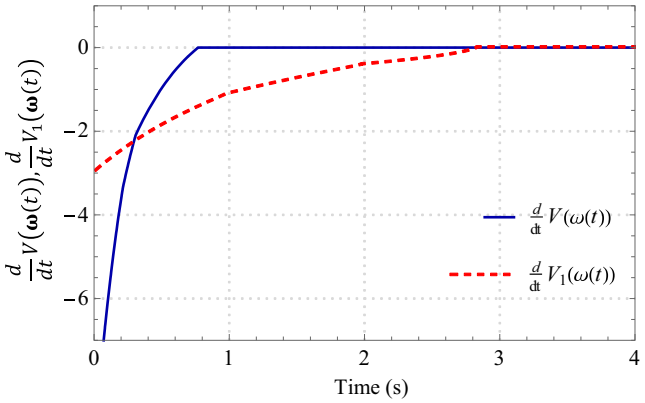

Fig. 13. Comparison of the rate of energy functions.

Table 7
Comparitive results for the dissipation rate of the energy function.

Feedback control technique	Parameter variations and exogenous disturbances	Energy function	Dissipation rate of the energy function
Eq. (14)	Eqs. (23a) and (24a)	$V(\omega(t)) = \frac{1}{2}\sum_1^3 \omega_i^2(t)$	$\frac{d}{dt}V(\omega(t)) \le -\sum_1^3(\alpha_i\psi_i(t) + \eta_i)\omega_i^2(t) - \sum_1^3(\gamma_i\psi_i(t) + \beta_i)\lvert\omega_i(t)\rvert$
Eq. (28)	Eqs. (23a) and (24a)	$V_1(\omega(t)) = \frac{1}{2}\sum_1^3 \omega_i^2(t)$	$\frac{d}{dt}V_1(\omega(t)) \le -\left(\frac{1}{2}\right)^{\frac{p+1}{2}}\left(\frac{1}{2}\sum_1^3\omega_i^2(t)\right)^{\frac{p+1}{2}}$

Table 8
Comparison of the convergence time in simulations.

Proposed FTC (14)				FTC in [20]			
Figure No.	Parameter variations	Exogenous disturbances	Convergence time	Figure No.	Parameter variations	Exogenous disturbances	Convergence time
6(a)	Does not vary	No disturbances	$t = 0.47s$	11	Does not vary	No disturbances	Diverge
10(a)	Eq. (23a)	Eq. (24a)	$t = 0.76s$	12(a)	Eq. (23a)	Eq. (24a)	$t = 2.6s$
10(b)	Eq. (23b)	Eq. (24b)	$t = 0.68s$	12(b)	Eq. (23b)	Eq. (24b)	Diverge

Conclusions

This article designs a novel robust finite-time feedback control law. It describes the chaotic finance model properties and proposes a controller that flourishes finite-time globally stable closed-loop supported by the established theoretical analysis. The proposed controller scheme accomplishes oscillation-free and faster convergence of the state variables to the equilibrium point in the presence of parameter variations and exogenous disturbances. The closed-loop theoretical and computer simulation analysis affirms the robust performance. A comparative performance study verifies that the proposed finite-time feedback control algorithm is superior in smoothness, robustness, convergence rate, and disturbance rejection. Time of convergence remains lesser than the upper bound of the finite time of convergence. The upper bound of the finite-time is insensitive to the parameter variations and exogenous disturbances. Therefore, the closed-loop is robust.

The research team will study the proposed controller's performance for the possible Markovian jumps in the chaotic finance model and modify the controller if needed.

Compliance with Ethics Requirements

This article does not contain any studies with human or animal subjects.

Declaration of Competing Interest

The authors declare that they have no known competing financial interests or personal relationships that could have appeared to influence the work reported in this paper.

Appendix A. [30]

$$\begin{cases} u_1(t) = \alpha_1(\omega_1(t) - \omega_1(t-\tau_1)) \\ u_2(t) = \alpha_2(\omega_2(t) - \omega_2(t-\tau_2)) \\ u_3(t) = \alpha_3(\omega_3(t) - \omega_3(t-\tau_3)) \end{cases}$$

where τ_1, τ_2, and τ_3 are the time-delays, and $\boldsymbol{\alpha} = diag[\alpha_i,\ \ i = 1,2,3]$ is a matrix of the feedback gain.

Appendix B. [32]

$$u_1(t) = \frac{-\omega_{e3} - \left(\omega_y(t) + \omega_{e2} - \eta_1\right)(\omega_x(t) + \omega_{e1}) - \beta\left(\frac{1}{2}\omega_x^2(t)\right)^p}{\omega_x(t)}$$

$$u_2(t) = k_1\omega_y(t), u_2(t) = k_1\omega_z(t)$$

where

$$k_1 = \frac{\begin{pmatrix} \omega_x(t)\omega_z(t) + \omega_{e3}(t)\omega_x(t) + \left(\omega_y(t) + \omega_{e2} - \eta_1\right)(\omega_x(t) + \omega_{e1})\omega_x(t) - \beta\left(\frac{1}{2}\omega_x^2(t)\right)^p + \omega_y(t) \\ -\eta_2\omega_y(t)\left(\omega_y(t) + \omega_{e2}\right) - (\omega_x(t) + \omega_{e1})^2\omega_y(t) - (\omega_x(t) + \omega_{e1})\omega_z(t) - \eta_3\omega_z(t)(\omega_z(t) + \omega_{e3}) + \beta(V(\boldsymbol{Y}(t)))^p \end{pmatrix}}{\omega_x^2(t) + \omega_z^2(t)},$$

$\{\omega_x(t) = \omega_1(t) - \omega_{e1}, \omega_y(t) = \omega_2(t) - \omega_{e2}, \omega_z(t) = \omega_3(t) - \omega_{e3},$ $\boldsymbol{Y}(t) = [\,\omega_x(t) \quad \omega_y(t) \quad \omega_z(t)\,]^T$, and $\beta > 0$, $0 < p < 1$ are any two real constants.

Appendix C. [33]

$$\begin{cases} u_4(t) = k_1\dot{\omega}_1(t) = k_1\left(\omega_2(t) + \frac{1}{\eta_2} - \eta_1\right)\omega_1(t) - \frac{\eta_4}{\eta_2}\omega_1(t) \\ \qquad\qquad -\eta_4\omega_1(t)\omega_2(t) - \eta_4\omega_4(t), \\ u_1(t) = u_2(t) = u_3(t) = 0, \end{cases}$$

where $\eta_i, i = 1,2,3,4$ are the positive parameters of the proposed hyperchaotic finance model, and k_1 is a feedback gain.

Appendix D. [34]

$$\boldsymbol{u}(t) = \boldsymbol{\alpha}(\boldsymbol{\omega}(t) - \boldsymbol{\omega}_e) - \boldsymbol{\beta}(\boldsymbol{\omega}(t-\tau) - \boldsymbol{\omega}_e)$$

where $\boldsymbol{\omega}_e = (\omega_{e1}, \omega_{e2}, \omega_{e3})$ is the equilibrium point of the chaotic financial system, $\boldsymbol{\alpha} = diag[\alpha_i, i = 1,2,3]$ and $\boldsymbol{\beta} = diag[\beta_i, i = 1,2,3]$ are the feedback gain matrices.

Appendix E. [36]

$$u_1(t) = \alpha_1\omega_1(t), u_2(t) = u_3(t) = u_4(t) = 0$$

and α_1 is a feedback gain.

Appendix F. [37]

$$\begin{cases} u_1(t) = -\omega_3(t) - \left(\omega_2(t) - \widehat{\eta}_1(t)\right)\omega_1(t) - \omega_4(t) - \alpha_1\omega_1(t) \\ u_2(t) = -1 + \widehat{\eta}_2(t)\omega_2(t) + \omega_1^2(t) - \alpha_2\omega_2(t) \\ u_3(t) = \omega_1(t)\widehat{\eta}_3(t)\omega_3(t) - \alpha_3\omega_3(t) \\ u_3(t) = 0.05\omega_1(t)\omega_3(t) - \widehat{\eta}_4(t)\omega_3(t) - \alpha_4\omega_4(t) \end{cases}$$

where $\widehat{\eta}_i(t), i = 1,2,3,4$ are the uncertain parameters of the proposed hyperchaotic finance model and $\boldsymbol{\alpha} = diag[\alpha_i, i = 1,2,3,4]$ is the gain matrix.

Appendix G. [38]

$$u_1(t) = \begin{cases} \widehat{k}(t)\omega_1(t) - \frac{\xi(V_1(\boldsymbol{\omega}(t)))^p}{\omega_1(t)}, \text{if}\,\omega_1(t) \neq 0, \\ 0, \text{if}\,\omega_1(t) = 0 \end{cases}$$

where $\xi > 0$, $0 < p < 1$ are any positive real constants, $\boldsymbol{\omega}(t) = \omega_1^2(t) + \omega_2^2(t) + \omega_3^2(t)$, $V_1(\boldsymbol{\omega}(t)) = \frac{1}{2}\omega_1^2(t) + V_0(\omega_2(t), \omega_3(t))$, and V_0 is a positive definite function of $(\omega_2(t), \omega_3(t))$. The unknown controller parameter $\widehat{k}(t)$ is adapted according to the law, $\dot{\widehat{k}}(t) = -\lambda\boldsymbol{\omega}(t)$, and $\lambda \in R^+$.

Appendix H. [39]

$$\boldsymbol{u}(t) = \boldsymbol{\alpha}(\boldsymbol{\omega}(t) - \boldsymbol{\omega}_e(t)) + \boldsymbol{\beta}(\boldsymbol{\omega}(t-\tau) - \boldsymbol{\omega}_e(t))$$

where $\boldsymbol{\alpha} = diag[\alpha_i, i = 1,2,3]$ and $\boldsymbol{\beta} = diag[\beta_i, i = 1,2,3]$ are the matrices of feedback gains, τ is the time-delay, and $\boldsymbol{\omega}_e(t) = (\omega_{e1}(t), \omega_{e2}(t), \omega_{e3}(t))$ is one of the unstable equilibrium points.

Appendix I. [40]

$$\boldsymbol{u}(t) = G(\boldsymbol{\alpha} + \Delta\boldsymbol{\alpha})(\boldsymbol{\omega}(t) - \boldsymbol{\omega}_e(t)) + G(\boldsymbol{\beta} + \Delta\boldsymbol{\beta})(\boldsymbol{\omega}(t-\tau) - \boldsymbol{\omega}_e(t))$$

where the matrix $G = diag[l_1, l_2, \cdots, l_m]$ specify the fault effects, $\boldsymbol{\omega}_e(t) = (\omega_{e1}(t), \omega_{e2}(t), \omega_{e3}(t))$ is one of the unstable equilibrium point, $\boldsymbol{\alpha} = diag[\alpha_i, i = 1,2,3]$ and $\boldsymbol{\beta} = diag[\beta_i, i = 1,2,3]$ represent the gain matrices, and $\Delta\boldsymbol{\alpha} = diag[\Delta\alpha_i, i = 1,2,3]$ and $\boldsymbol{\beta} = diag[\Delta\beta_i, i = 1,2,3]$ denote the gains fluctuation with appropriate dimension.

References

[1] Devaney RL. Chaotic Dynamical System. 2nd ed. New York: Addison-Wesley; 1989.
[2] Kwietniak D, Oprocha P. Topological entropy and chaos for maps induced on hyperspaces. Chaos Solit Fract 2007;33:76–86.
[3] Mouelas N, Fozin TF, Kengne R, et al. Extremely rich dynamical behaviors in a simple nonautonomous Jerk system with generalized nonlinearity: Hyperchaos, intermittency, offset-boosting and multistability. Int J Dyn Control 2020;8:51–69.
[4] Lai Q, Nestor T, Kengne J, Zhao X. Coexisting attractors and circuit implementation of a new 4D chaotic system with two equilibria. Chaos Solit Fractals 2018;107:92–102.
[5] Sajjadi SS, Baleanu D, Jajarmi A, Pirouz HM. A new adaptive synchronization and hyperchaos control of a biological snap oscillator. Chaos Solit Fract 2020;138:1–13.
[6] Aghababa MP. Adaptive switching control of uncertain fractional systems: Application to Chua's circuit. Int J Adapt Cont Signal Process 2019;32 (8):1206–21.
[7] Lin CJ, Yang SK, Yau HT. Chaos suppression control of a coronary artery system with uncertainties by using variable structure control. Comp Math Appl 2012;64(5):988–95.
[8] Zang X, Iqbal S, Zhu Y, Liu X, Zhao J. Applications of chaotic dynamics in robotics. Int J Adv Robot Syst 2017;13(60):1–17.
[9] Köse E. Controller design by using nonlinear control methods for satellite chaotic system. Elect Eng 2017;99:763–73.
[10] Aroudi AE, Mandal K, Giaouris D, Banerjee S. Self-compensation of DC-DC converters under peak current mode control. Elect Lett 2017;53(3):345–6.
[11] Zhou L, Chen F. Chaotic dynamics for a class of single-machine-infinite bus power system. J Vib Chaos 2018;24(3):582–7.
[12] Iqbal A, Singh K. Chaos control of permanent magnet synchronous motor using simple controllers. Trans Intit Measur Control 2019;41(8):2352–64.
[13] Shi K, Wang J, Zhong S, Tang Y, Cheng J. Non-fragile memory filtering of T-S fuzzy delayed neural networks based on switched fuzzy sampled-data control. Fuzzy Set Syst 2020;394(1):40–64.
[14] Shi K, Wang J, Tang Y, Zhong S. Reliable asynchronous sampled-data filtering of T-S fuzzy uncertain delayed neural networks with stochastic switched topologies. Fuzzy Set Syst 2020;381(1):1–25.
[15] Meskine K, Khaber F. Robust backstepping control for uncertain chaotic multi-inputs multi-outputs systems using type 2 fuzzy systems. Trans Intit Measur Control 2018;40(15):4153–65.
[16] Luo J, Li M, Liu X, Tian W, Zhong S, Shi K. Stabilization analysis for fuzzy systems with a switched sampled-data control. J Franklin Inst 2020;357:39–58.
[17] Singh PP, Singh KM, Roy BK. Chaos control in biological system using recursive backstepping sliding mode control. The Eur Phys J: Spec Topics 2018;227:791–1746.
[18] Shi K, Wang J, Zhong S, Tang Y, Cheng J. Hybrid-driven finite-time H∞ sampling synchronization control for coupling memory complex networks with stochastic cyber-attacks. Neurocomputing 2020;387:241–54.
[19] Pan Y, Bobtsov A, Darouach Joo YH. Learning from adaptive control under relaxed excitation conditions. Int J Adapt Cont Sig Process 2019;33 (12):1723–5.
[20] Du-Qu W, Bo Z. Controlling chaos in permanent magnet synchronous motor based on finite-time stability theory. Chinese Phys B 2009;18(4):1399–405.
[21] Aghababa MP, Aghababa HP. Stabilization of gyrostat system with dead-zone nonlinearity in control input. J Vib Control 2014;20(15):2378–88.
[22] Luo R, Su H. Finite-time control and synchronization of a class of systems via the twisting controller. Chinese J Phys 2017;55(6):2199–207.
[23] Sun K, Qiu J, Karimi HR, Gao H. A novel finite-time control for nonstrict feedback saturated nonlinear systems with tracking error constraint. IEEE Tran Syst Man Cyber: Syst 2019:1–12. doi: https://doi.org/10.1109/TSMC.2019.2958072.
[24] Jiang B, Karimi HR, Kao Y, Gao C. Takagi-Sugeno model-based sliding mode observer design for finite-time synthesis of Semi-Markovian jump systems. IEEE Tran Syst Man Cyber: Syst 2019;49(7):1505–15.
[25] Jun-hai MS, Yu-shu C. Study of the bifurcation topological structure and the global complicated character of a kind of nonlinear finance system (II). Appl Math Mech 2001;22(11):1240–51.
[26] Jian JG, Deng XL, Wang JF. In: Globally exponentially attractive set and synchronization of a class of chaotic finance system. Lect. Notes Comput Sci 2009; 5551:253–261. Springer, Berlin.
[27] Gao Q, Ma J. Chaos and Hopf bifurcation of a finance system. Nonlinear Dyn 2009;58:209–16.
[28] Abraham CL, Chian Erico L, Rempel Rogers C. Complex economic dynamics: Chaotic saddle, crisis and intermittency. Chaos Solit Fract 2006;29:1194–218.
[29] Chena L, Chen G. Controlling chaos in an economic model. Phys A 2007;374:349–58.
[30] Chen WC. Dynamics and control of a financial system with time-delayed feedbacks. Chaos Solit Fract 2008;37:1198–207.
[31] Pyragas K. Continuous control of chaos by self-controlling feedback. Phys Lett A 1992;170:421–8.
[32] Wang Y, Ma J, Xu Y. Finite-time chaos control of the chaotic financial system based on control Lyapunov function. App Mech Mater 2011;55–57:203–8.
[33] Yu H, Cai G, Li Y. Dynamic analysis and control of a new hyperchaotic finance system. Nonlinear Dyn 2012;67:2171–82.
[34] Zhao M, Wang J. H∞ control of a chaotic finance system in the presence of external disturbances and input time-delay. Appl Math Comput 2014;233:320–7.
[35] Pontryagin LS, Boltyanskii VG, Gamkelidze RV, et al. The Mathematical Theory of Optimal Processes. Moscow: Nauka; 1983.
[36] Cao L. A four-dimensional hyperchaotic finance system and its control problems. J Cont Sci Engineering 2018, Article ID: 4976380, 12 pages doi. org/10.1155/2018/4976380.
[37] Jajarmi A, Hajipour H, Baleanu D. New aspects of the adaptive synchronization and hyperchaos suppression of a financial model. Chaos Solit Fract 2017;99:285–6.
[38] Ma C, Tian Y, Qu Z. Finite time stability of finance systems with or without market confidence using less control input. Math Prob Engineering 2018, Article ID: 7149801, 15 pages.
[39] Xu E, Chen Y, Yang J. Finite-time H∞ control for a chaotic finance system via delayed feedback. Syst Sci Cont Eng 2018;6(1):467–76.
[40] Harshavarthini S, Sakthivel R, Mac Y-K, Muslim M. Finite-time resilient fault-tolerant investment policy scheme for chaotic nonlinear finance system. Chaos Solit Fract 2020;131:1–8.
[41] Lyapunov AM. The general problem of the stability of motion (translated into English by Fuller AT). Int J Control 1992;1992(55):531–773.
[42] Yu X, Yin J, Khoo S. Generalized Lyapunov criteria on finite-time stability of stochastic nonlinear systems. Automatica 2019;107:183–9.
[43] Grebogi C, Ott E, Yorke JA. Chaos, strange attractors, and fractal basin boundaries in nonlinear dynamics. Science 1987;238(4827):632–8.
[44] Muñoz-Cobo JL, Verdu G, Pereira C. Dynamic reconstruction and Lyapunov exponents from time series data in boiling water reactors, application to BWR stability analysis. Ann Nucl Energy 1992;19:223–35.
[45] Schuster GH. Deterministic Chaos: An Introduction. New York: Wiley-VCH; 1995.
[46] Hénon M. On the numerical computation of Poincaré maps. Physica D 1982;5:412–4.
[47] Vallejo JC, Sanjuan MAF. Predictability of Chaotic Dynamics: A Finite-Time Lyapunov Exponents Approach. 2nd ed. Springer; 2017.
[48] Ahmad I, Shafiq M. A generalized analytical approach for the synchronization of multiple chaotic systems in the finite-time. Arabian J Sci Eng 2020;45 (3):2297–315.
[49] Khalil HK. Nonlinear Systems. New Jersey: Prentice-Hall; 2002.
[50] Burden RL, Faires JD. Numerical Analysis. 9th ed. Boston, USA: Brooks/Cole; 2011.
[51] Yang WY, Cao W, Chung TS, Morris J. Applied Numerical Methods using MATLAB. John Wiley & Sons; 2005.
[52] Guan C, Fei Z, Karimi HR, Shi P. Finite-time synchronization for switched neural networks via quantized feedback control. IEEE Tran Syst Man Cyber: Systems 2019:1–12. doi: https://doi.org/10.1109/TSMC.2019.2917497.
[53] Ren H, Xong G, Karimi HR. Asynchronous finite-time filtering of networked switched systems and its application: An event-driven method. IEEE Tran Circ Syst I: Regular paper 2019;66(1):391–402.
[54] Wang N, Karimi HR, Li H, Su SH. Accurate trajectory tracking of disturbed surface vehicles: a finite-time control approach. IEEE/ASME Trans Mech 2019;24(3):1067–74.